Ferromagnetic Materials

DOI: 10.1002/anie.201006672

Spaced Heterometallic 3d–4f Magnetic Chains from the Pseudo-One-Dimensional $Na_2LnMnO(AsO_4)_2$ Series: Stepped Magnetization in the $Na_2GdMnO(AsO_4)_2$ Ferromagnet**

J. Palmer West, Wendy L. Queen, Shiou-Jyh Hwu, and Katherine E. Michaux*

Mixed first-row transition-metal (3d) and lanthanide (4f) oxides have long been an attractive area of research due to their diverse electronic and magnetic properties. In the pursuit of quantum magnetic solids, nanostructures based on heterometallic 3d–4f ions have been an emerging subject of interest.[1,2] Among the most studied are molecular-based magnetic systems, such as single-molecule magnets (SMMs) and single-chain magnets (SCMs). The f-block elements are magnetically appealing because they possess significant orbital contributions (with the exception of f^n, $n = 0$, 7, 14) and have large spin ground states (S) leading to sizable energy barriers (defined by $|D|S^2$, where D is a zero-field splitting parameter), which are crucial for slow relaxation of magnetization, and subsequently to an increase in the blocking temperatures below which these materials behave as single-domain magnets.[2,3]

In extended solids, structural spacing of magnetic nanostructures could conceivably facilitate the formation of single-domain magnetic sublattices and in turn lead to quantized magnetic phenomena. This task is rather challenging, as extended systems have a strong propensity to form 3D magnetic order owing to the presence of various exchange pathways. The low transition temperatures associated with 3d–4f SMMs[2] and SCMs[3a,c] ($T_C < 5$ K), which are partly due to phonon interactions induced by soft organic ligands,[5] have inspired us to employ closed-shell, nonmagnetic inorganic oxyanions instead of organic ligands to "encapsulate" magnetic nanostructures.[4] Our ultimate goal is to establish "true" structural confinement in extended solids, as the use of rigid, inorganic, encapsulating ligands could potentially produce the magnetic phenomena associated with spin confinement at higher temperatures. Through exploratory synthesis we have discovered the first 3d–4f extended solids exhibiting magnetization steps possibly originating from better confined magnetic nanostructures.

The new family of pseudo-one-dimensional (1D) compounds $Na_2LnMnO(AsO_4)_2$ exhibits $[MnO_4]_\infty$ ferromagnetic chains that are spaced further apart than those in the reported $Na_3LnMn_3O_3(AsO_4)_3$ series.[1] The Gd^{3+} derivative in the present series reveals fascinating magnetic anomalies, including stepped magnetization and multiple-spin dynamics. Herein, we report the synthesis, structure, and magnetic properties of new 3d–4f solids $Na_2LnMnO(AsO_4)_2$ (Ln = Sm^{3+} **1**, Gd^{3+} **2**, Dy^{3+} **3**) and their structural comparison with the $Na_3LnMn_3O_3(AsO_4)_3$ (Ln = La^{3+} **4**, Sm^{3+} **5**, Gd^{3+} **6**) series.[1] These two families will be referred to as 2112 and 3133, respectively.

We have demonstrated that these intriguing magnetic anomalies in gadolinium derivative **2** can possibly be attributed to its structurally spaced magnetic chains. These spaced chains would induce a low ratio of interchain to intrachain magnetic couplings. But magnetic studies of **2** suggest that the interchain magnetic interactions are likely strong enough to rule out any possible superparamagnetic-like behavior derived from the $[MnO_4]_\infty$ chains. On the path to achieving quantum magnetic solids, we do see magnetic effects that are thought to be associated with structural confinement, as discussed below. From the point of view of structure–property correlation, the stepped magnetization and frequency-dependent out-of-phase AC susceptibility are significant, as these two phenomena have never before been observed in a quasi-one-dimensional, 3d–4f extended system. Owing to the lack of sizable crystals and yields of the samarium and dysprosium analogues, the magnetic comparisons and correlation studies will focus on the 2112-Gd (**2**) and 3133-Gd (**6**) derivatives.

Compound **2** forms amber-brown columnar crystals. The 1D $[MnO_4]_\infty$ chains are made of MnO_6 octahedra that are fused together through opposite edges and extend parallel to channels containing sodium ions (Figure 1a). The 1D $[MnO_4]_\infty$ chains are capped by GdO_8 units in an alternating fashion (Figure 1b). The chemical content of the crystal used for data collection was verified by EDX, and the oxidation states of the Mn^{3+} ions were confirmed by bond valence sum (BVS) calculations (Table S4 in the Supporting Information).[6]

Structurally, as shown in Figure 2, the chains in **2** are separated further by Gd^{3+} ions than in **6**, thus resulting in a longer Mn-O-As-O-Gd-O-Mn linkage than Mn-O-As-O-Mn in **6**. In fact, the interchain Mn···Mn distances are significantly longer in **2** (8.647(1) and 9.037(2) Å) than in **6** (5.545(1) Å).

[*] J. P. West, Dr. W. L. Queen, Dr. S.-J. Hwu
Department of Chemistry, Clemson University
Clemson, SC 29634-0973 (USA)
Fax: (+1) 864-656-6613
E-mail: shwu@clemson.edu
K. E. Michaux
Department of Chemistry
Virginia Polytechnic Institute and State University
Blacksburg, VA 24061 (USA)

[**] This work was supported by the National Science Foundation (DMR-0706426). Funds from the NSF for the purchase of a SQUID magnetometer (CHE-9808044) and of an X-ray diffractometer (ESR-9108772, CHE-9207230, 9808165) are also gratefully acknowledged. Ln = Sm, Gd, Dy.

Supporting information for this article is available on the WWW under http://dx.doi.org/10.1002/anie.201006672.

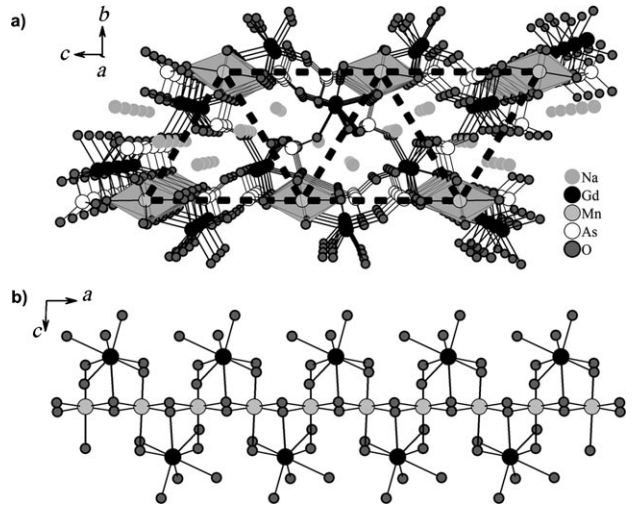

Figure 1. a) Projected view of the crystal structure of **2** showing well-separated $[MnO_4]_\infty$ ferromagnetic chains (8.65–9.04 Å) arranged in a triangular relationship as highlighted by dotted lines. b) Ball-and-stick representation showing the 3d–4f heterometallic chain comprising the $[MnO_4]_\infty$ octahedral chain alternately capped by GdO_8 units.

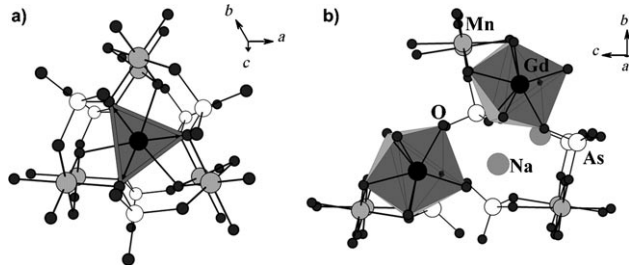

Figure 2. Mixed polyhedral and ball-and-stick drawings showing the connectivity of the parallel $[MnO_4]_\infty$ chains for a) $Na_3GdMn_3O_3(AsO_4)_3$ (**6**)[1] and b) $Na_2GdMnO(AsO_4)_2$ (**2**). Intrachain separations in **2** [Å]: Mn(1)–Mn(2) 2.8814(6), Gd–Mn(1) 3.3697(7), and Gd–Mn(2) 3.4847(8).

As can be seen from the partial structure of **6** in Figure 2a, the lanthanide ion is shared by three neighboring $[MnO_4]_\infty$ chains that form a Gd-centered Mn-O-As-O-Mn framework. The Gd^{3+} cation resides in the center of a tricapped trigonal prism (gray polyhedron in Figure 2a), giving rise to the GdO_9 coordination. In **2**, the neighboring Gd-capped $[MnO_4]_\infty$ chains are interconnected through As^{5+} ions extending along the *bc* plane, thus creating $[MnO_4]_\infty$ chains that are spaced further apart. This variation, attributed in part to an increased Gd/Mn ratio, could potentially dictate the strength of interchain couplings through possible competing pathways, including Mn-O···O-Mn super superexchange. Intuitively, we expect that the magnetic interactions are dictated predominately by intrachain interactions.

The magnetic properties of **2** were investigated in both direct and alternating current (DC and AC) modes. The inverse magnetic susceptibility (χ_M^{-1}) and magnetic moment (μ) versus temperature (T) curves (Figure 3 and Figures S1, S2 in the Supporting Information) clearly indicate the presence of a ferromagnetic (FM) transition at 20 K. As observed in the 3133 series, the FM interaction originates from the $[MnO_4]_\infty$ magnetic chains and can be rationalized in terms of the Mn-O^b-Mn bridging angles. Both 2112 and 3133 have two different angles (Table S3 in the Supporting Information) through bridging oxygen atoms ($O(1)^b$ and $O(2)^b$); one is significantly larger than 90° and the other is nearly orthogonal, that is, 100.8(2)°/93.8(2)° and 106.4(7)°/91.7(6)° for **2** and **6**, respectively. It is well known that if the two involved O^b p orbitals are completely or nearly orthogonal, a more significant FM contribution for the spins of the two bridged Mn^{3+} ions is expected, or else the single O^b p orbital provides a superexchange pathway giving rise to antiferromagnetic (AFM) coupling.[7] With the variance in ∡Mn-O^b-Mn, a possible competition between AFM and FM coupling is anticipated, and the end result is a FM intrachain coupling between Mn^{3+} centers (see below).

The variable-temperature (T) magnetic susceptibility (χ) of **2** displays Curie–Weiss behavior in the high-temperature region (50 to 300 K), and a fit gives an effective magnetic moment (μ_{eff}) of 9.3(5) μ_B, which is in good agreement with the spin-only moment of 9.3 μ_B expected from high-spin Mn^{3+} (d^4) and Gd^{3+} ($L=0$, f^7). The relatively small positive Weiss constant (θ) of 11.1(4) K (Table S5 in the Supporting Information) suggests a weakened FM, intrachain coupling compared to **6** ($\theta=38.5(5)$ K). The μ versus T and $d\mu/dT$ plots (Figure 3 top inset) suggest a FM transition at $T_C \approx 20$ K,

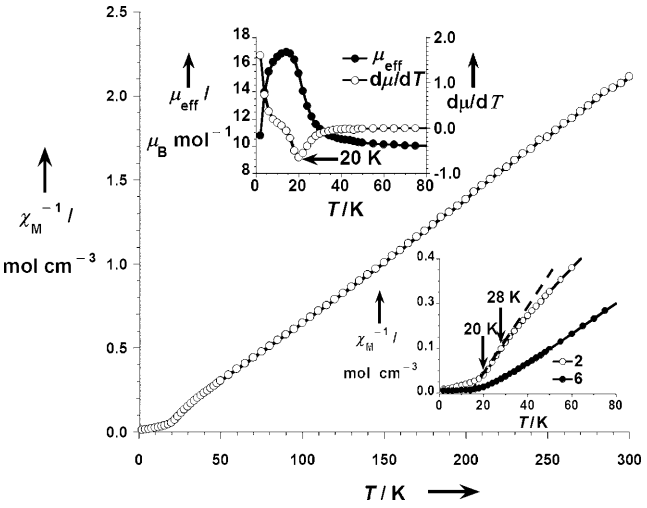

Figure 3. Temperature dependence of the inverse molar magnetic susceptibility (χ_M^{-1}) of a ground powder of **2** at 0.5 T. The top inset shows μ and $d\mu/dT$ vs. T. The bottom inset shows χ_M^{-1} of both **2** and **6** for comparison. The dotted line is drawn to show the change of slope in **2**.

which is on the same order of magnitude as θ. At low temperature, there is an abrupt decrease in μ, which likely signifies the onset of weak AFM interchain interactions. The field cooling and zero-field cooling (FC/ZFC) curves (Figure S8 in the Supporting Information) indicate some irreversibility below T_C, which is overcome at higher applied fields. Such behavior is typical of glassy and FM materials but does not imply low dimensionality. At low applied fields (less than

0.01 T), the FC susceptibility data reveals a slight decrease at low temperatures (below 4 K), indicative of weak interchain AFM coupling consistent with the ZFC curve at 0.01 T, which shows, as expected, a decrease when the temperature is reduced to below 10 K.

Figure 4 shows the field-dependent magnetization of one aligned single crystal of **2**. The plot reveals that the saturation of magnetization occurs faster along the *b* and *c* axes than

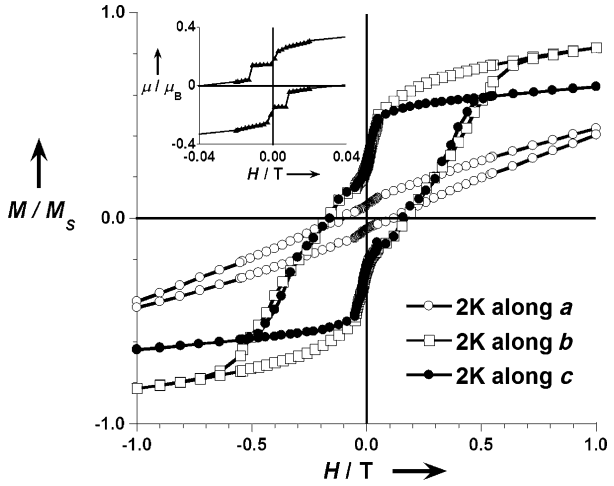

Figure 4. Magnetization (M/M_S) versus magnetic field of one oriented single crystal of **2** along the *a*, *b*, and *c* axes at 2 K. A normalized magnetization (M/M_s) is plotted because the crystal is too small to acquire an accurate mass. The inset shows *M* vs. *H* for a powder sample of selected crystals.

along the *a* axis. This finding is indicative of magnetocrystalline anisotropy within the *bc* plane, instead of along the chain axis, through a possible influence of 4f Gd^{3+} ions.

There are several unusual magnetic features observed for **2** that are believed to be associated with the structural confinement of the $[MnO_4]_\infty$ chains. First, the field-dependent data reveal magnetization steps (Figure 4 inset), which are likely a result of weak interchain AFM couplings. These steps are diminished above an applied field of approximately 0.01 T at 2 K, thus indicating a possible metamagnetic transition. This phenomenon has similarly been observed in some of the recent examples, such as $MH_2P_2O_7$[8a] and $LiM_2H_3(P_2O_7)_2$[8b] (M = Ni, Co), in which the magnetic chains are reportedly quasi-one-dimensional. Second, the AC magnetic susceptibility (Figure 5 and Figure S9 in the Supporting Information) shows a rather complicated frequency dependence, where the nonzero χ'' signal covers a broad range of temperatures (ca. 8–19 K). This broad range seems larger than typical for most spin-glass-type systems. The possible presence of multiple-spin dynamics makes it difficult to assess the actual size of the frequency dependence. Furthermore, although the 3d chains in **2**, like in $Ca_3Co_2O_6$,[9] exhibit an interchain triangular arrangement (Figure 1a), the magnetization anomalies are unique in that the magnetization steps ($\leq$ 6 K) are observed outside the temperature range in which the spin dynamics occur. We speculate that the step-like magnetization features (see Figure 4 inset and Figures S4–7 in the Supporting

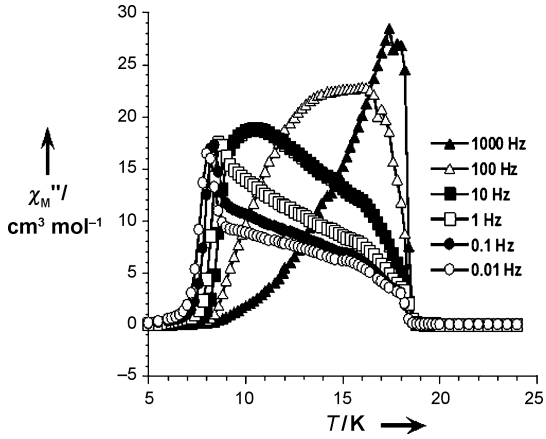

Figure 5. Temperature dependence of the out-of-phase (χ'') AC magnetic susceptibility from a ground powder of selected crystals of **2** at various frequencies with a 3×10^{-4} T AC field and no applied DC field.

Information) are the result of a spin-flip transition from AFM to FM, likely owing to weak coupling between the chains (or lack thereof above 8 K). We also speculate that the frequency dependence could be due to some type of disordered magnetic states inherent to weak interchain couplings and potentially also to the influence of the Gd^{3+} exchange interactions in relation to the Mn^{3+} FM order.

In light of the potential effects of Gd–Mn interactions, we note the similar multiple-spin dynamics observed in the quasi-two-dimensional Gd_2CuO_4 phase.[10] The double peak anomaly in Gd_2CuO_4 was attributed to the influence of Gd–Gd (4f–4f) exchange interactions on the Cu^{2+} (3d) magnetic sublattice. The influence of the 4f exchange interactions causes the polarization of a canted moment, thus breaking the 3D magnetic order of Cu^{2+} spins. By the same token, the magnetic interactions associated with Gd^{3+} could disrupt intrachain magnetic ordering between Mn^{3+} centers in **2**.

Finally, it is evident that compound systems containing lanthanide ions (Ln^{3+}) also offer synthetic advantages with regard to the isolation of extended families of structurally related phases. Such studies facilitate the systematic investigations of structure–property correlation that often lead to the recognition of magnetic patterns and, in turn, to the rationalization of the coupling mechanism and synthetic advances. To acquire direct information on the magnetic excitations occurring in the 2–30 K range, we could in principle use UV/Vis spectra to obtain information on the crystal-field effects on the individual lanthanide ions, anisotropic magnetic measurements down to very low temperature on pure and diamagnetically substituted derivatives (such as La^{3+}, which has not yet been successful), and EPR spectra and, for magnetic anisotropy, reflection and refraction of spin-flip neutron experiments on single crystals to provide much additional insight into the low-lying orbitals. Field-dependent heat capacity measurements should also aid in elucidating the complex magnetic behavior exhibited in **2**. We will also carry out torque measurements and theoretical calculations to investigate the magnetoanisotropy of the series.

In conclusion, the 2112 series, like the previously reported 3133 series, contains Ln-capped $[MnO_4]_\infty$ magnetic chains.

Compound **2** reveals intriguing magnetic anomalies that arise from competing multiple magnetic dynamics and, for the first time, stepped magnetization below the Curie temperature $T_C \approx 20$ K. We believe that anomalies can be attributed to an increased spacing between $[MnO_4]_\infty$ FM chains, which weakens interchain couplings in comparison to **6**. The displayed low-dimensional magnetic behavior along with the magneto-aniostropy within the *bc* plane seem to suggest that the Gd^{3+} ions have an important structural or magnetic influence on the magnetic properties of **2**. We anticipate that continued study of these systems will further our understanding and lead to the discovery of more interesting magnetic phenomena of technological and theoretical importance involving low-dimensional, 3d–4f heterometallic magnetic solids.

Experimental Section

2: A mixture of Na_2O_2, Gd_2O_3, Mn_2O_3, and As_2O_5 (2:1:1:2 molar ratio, total 0.25 g) was ground in a CsCl/NaCl mixed salt (ca. 0.75 g). The experimental procedures and the heating program are the same as reported in reference [1]. The yield of **2** is approximately 60 % of the crystalline phases; the remainder is primarily compound **6** (see Figures S10 and S11 in the Supporting Information). Sm^{3+} and Dy^{3+} analogues were also discovered; however, the crystal quality and yields were poor (see Tables S1–S3 in the Supporting Information for crystallographic data).

Crystal data for **2**: $Na_2GdMnO(AsO_4)_2$, brown columns, $M_r = 552.01$, monoclinic, space group $P2_1/n$ (no. 14), $a = 5.763(1)$, $b = 14.746(3)$, $c = 9.037(2)$ Å, $\beta = 92.66(3)°$, $V = 767.1(3)$ Å^3, $Z = 4$, $\rho_{calcd} = 4.780$ g cm^{-3}, $Mo_{K\alpha}$ ($\lambda = 0.71073$ Å) radiation, $2.65° < \theta < 29.66°$, final $R = 0.0365$, $R_W = 0.1006$, GOF = 0.906 (all data), 139 parameters. Further details on the crystal structure investigations may be obtained from the Fachinformationszentrum Karlsruhe, 76344 Eggenstein-Leopoldshafen, Germany (fax: (+49) 7247-808-666; e-mail: crysdata@fiz-karlsruhe.de), on quoting the depository number CSD-422219.

Magnetic measurements were carried out as described in reference [1].

Received: October 25, 2010
Revised: December 20, 2010
Published online: March 17, 2011

Keywords: chain structures · lanthanides · magnetic properties · transition metals · nanostructures

[1] J. P. West, S.-J. Hwu, W. L. Queen, *Inorg. Chem.* **2009**, *48*, 8439–8444.

[2] a) C. Benelli, D. Gatteschi, *Chem. Rev.* **2002**, *102*, 2369–2387, and references therein; b) A. Mishra, W. Wernsdorfer, S. Parsons, G. Christou, E. K. Brechin, *Chem. Commun.* **2005**, 2086–2088; c) M. Murugesu, M. Abhudaya, W. Wernsdorfer, K. Abboud, G. Christou, *Polyhedron* **2006**, *25*, 613–625; d) T. C. Stamatatos, S. J. Teat, W. Wernsdorfer, G. Christou, *Angew. Chem.* **2009**, *121*, 529–532; *Angew. Chem. Int. Ed.* **2009**, *48*, 521–524.

[3] a) K. Bernot, L. Bogani, A. Caneschi, D. Gatteschi, R. Sessoli, *J. Am. Chem. Soc.* **2006**, *128*, 7947–7956; b) R. Gheorghe, A. M. Madalan, J.-P. Costes, W. Wernsdorfer, M. Andruh, *Dalton Trans.* **2010**, *39*, 4734–4736.

[4] a) S. Wang, S.-J. Hwu, *J. Am. Chem. Soc.* **1992**, *114*, 6920–6922; b) S. Wang, S.-J. Hwu, *Inorg. Chem.* **1995**, *34*, 166–171; c) S. Wang, S.-J Hwu, J. A. Paradis, M.-H. Whangbo, *J. Am. Chem. Soc.* **1995**, *117*, 5515–5522; d) R. Mackay, T. A. Wardojo, S.-J. Hwu, *J. Solid State Chem.* **1996**, *125*, 255–260; e) S.-J. Hwu, *Chem. Mater.* **1998**, *10*, 2846–2859; f) M. Ulutagay-Kartin, K. M. S. G. Etheredge, G. L. Schimek, S.-J. Hwu, *J. Alloys Compd.* **2002**, *338*, 80–86; g) J. A. Clayhold, M. Ulutagay-Kartin, S.-J. Hwu, H.-J. Koo, M.-H. Whangbo, A. Voigt, K. Eaiprasertsak, *Phys. Rev. B* **2002**, *66*, 052403; h) S.-J. Hwu, M. Ulutagay-Kartin, J. A. Clayhold, R. Mackay, T. A. Wardojo, C. J. O'Connor, M. Krawiec, *J. Am. Chem. Soc.* **2002**, *124*, 12404–12405; i) M. Ulutagay-Kartin, S.-J. Hwu, J. A. Clayhold, *Inorg. Chem.* **2003**, *42*, 2405–2409; j) X. Mo, K. M. S. Etheredge, S.-J. Hwu, Q. Huang, *Inorg. Chem.* **2006**, *45*, 3478–3480; k) K. G. Sanjaya Ranmohotti, X. Mo, M. K. Smith, S.-J. Hwu, *Inorg. Chem.* **2006**, *45*, 3665–3670; l) R. Stern, I. Heinmaa, A. Kriisa, E. Joon, S. Vija, J. Clayhold, M. Ulutagay-Kartin, X. Mo, W. Queen, S.-J. Hwu, *Phys. B* **2006**, *378–380*, 1124–1125; m) W. L. Queen, S.-J. Hwu, L. Wang, *Angew. Chem.* **2007**, *119*, 5440–5443; *Angew. Chem. Int. Ed.* **2007**, *46*, 5344–5347.

[5] S. K. Ritter, *Chem. Eng. News* **2004**, *82*(50), 29–32, and references therein.

[6] I. D. Brown, D. Altermatt, *Acta. Crystallogr. Sect. B* **1985**, *41*, 244–247.

[7] J. Curély, *Monatsh. Chem.* **2005**, *136*, 1013–1036, and references therein.

[8] a) T. Yang, J. Ju, G. B. Li, S. H. Yang, J. L. Sun, F. H. Liao, J. H. Lin, J. Sasaki, N. Toyota, *Inorg. Chem.* **2007**, *46*, 2342–2344; b) T. Yang, S. Yang, F. Liao, J. Lin, *J. Solid State Chem.* **2008**, *181*, 1347–1353.

[9] a) H. Kageyama, K. Yoshimura, K. Kosuge, M. Azuma, M. Takano, H. Mitamura, T. Goto, *J. Phys. Soc. Jpn.* **1997**, *66*, 3996–4000; b) A. Maignan, V. Hardy, S. Hérbert, M. Drillon, M. R. Lees, O. A. Petrenko, D. M. Paul, D. Khomskii, *J. Mater. Chem.* **2004**, *14*, 1231–1236.

[10] a) A. A. Stepanov, P. Wyder, T. Chattopadhyay, P. J. Brown, G. Fillion, I. M. Vitebsky, A. Deville, B. Gaillard, S. N. Barilo, D. I. Zhigunov, *Phys. Rev. B* **1993**, *48*, 12979–12984; b) P. W. Klamut, *Phys. Rev. B* **1994**, *50*, 13009–13012; c) P. W. Klamut, K. Rogacki, A. Sikora, *J. Appl. Phys.* **1998**, *84*, 5129–5133.

